

## Preliminary refinement of rotation parameters of asteroids based on photogrammetric processing of on-orbit remote sensing images

Zhen Peng <sup>1,2</sup>, Xun Geng <sup>1,2,\*</sup>, Jiujiang Zhang <sup>1,2</sup>, Yuying Wang <sup>1,2</sup>

<sup>1</sup> College of Geographical Sciences, Faculty of Geographical Science and Engineering, Henan University, Zhengzhou, 450046, China - gengxun@henu.edu.cn

<sup>2</sup> Henan Industrial Technology Academy of Spatio-Temporal Big Data, Zhengzhou, Henan, China

**Keywords:** Asteroid, Rotation parameters, Forward intersection, Exterior orientation

### Abstract:

In recent years, asteroid exploration has become an important research direction in the field of deep space exploration. The weak gravitational environment of asteroids, as well as their complex topographic, geomorphic, and dynamic characteristics, pose significant technical challenges to surface exploration. The determination of high-precision asteroid rotation parameters is a fundamental requirement for engineering implementation and scientific research in deep space exploration missions. These parameters provide key information for establishing the asteroid coordinate system, which supports the transformation between the inertial frame and the body-fixed frame. Although traditional ground-based observation methods (such as light curve inversion) can provide preliminary estimates of rotation parameters, their accuracy is insufficient to meet the requirements of high-resolution remote sensing mapping and 3D reconstruction. Therefore, developing refinement methods for rotation parameters based on on-orbit remote sensing images has become a key technical approach. This paper proposes a preliminary refinement method for asteroid rotation parameters based on minimizing the residuals of forward intersection. First, rigorous geometric model incorporating the right ascension and declination is constructed, and the rotation parameters are gradually optimized through a "brute-force" search strategy. Experiments using on-orbit remote sensing images of Ceres, Vesta, and Ryugu asteroids verify the robustness and feasibility of the proposed method. The experimental results show that the proposed method can effectively refine the rotation parameters and remain stable even in the presence of initial orbit-determination errors.

### 1. Introduction

In recent years, asteroid exploration has emerged as a prominent focus within the field of deep space exploration. To investigate the primordial material composition and evolutionary history of the solar system, major space agencies worldwide have conducted numerous exploration missions targeting various asteroids (Lauretta et al., 2015; Preusker et al., 2016; Rayman and Mase, 2014; Tsuda et al., 2019). The exploration of asteroid surfaces presents significant technical challenges due to their weak gravitational environments and complex topographic, geomorphic, and dynamic characteristics. When approaching an unknown celestial body, one of the primary tasks is to establish a body-fixed frame (Burmeister et al., 2018). The high-precision determination of asteroid rotation parameters constitutes a fundamental requirement for both engineering implementation and scientific research in deep space exploration missions. These parameters, serving as essential elements for establishing the asteroid coordinate system, provide the foundation for coordinate transformation between the Inertial Frame and the Body-Fixed Frame. High-accuracy rotation parameters are prerequisite for conducting asteroid mapping and mission planning in exploration missions.

The acquisition of precise rotation parameters enables accurate geometric correction of asteroid remote sensing images, facilitates reliable trajectory design for orbiting and landing operations, and supports comprehensive scientific investigations (Roatsch et al., 2017). Furthermore, these parameters play a crucial role in understanding the asteroid's

thermal environment, internal structure, and evolutionary processes. The rotation parameters play a crucial role in determining the direction of the gravity field and serve as a fundamental reference for gravity field modelling (Konopliv and Sjogren, 1995). Methodologies for accurate determination of rotational parameter has therefore become an essential research direction in planetary science and space exploration (Lauretta et al., 2017).

The determination of asteroid rotation parameters serves as a fundamental prerequisite for deep space exploration missions, where their accuracy critically influences geometric positioning of remote sensing data and navigation control performance (Miller et al., 2002). Although conventional ground-based observation methods (e.g., light curve inversion) can provide initial estimates of rotation parameters, their precision remains insufficient for high-accuracy photogrammetric processing and engineering applications. Representative studies demonstrate these limitations: Drummond et al. (1998) determined Ceres' rotational axis orientation as right ascension  $333^{\circ} \pm 2^{\circ}$  and declination  $43^{\circ} \pm 2^{\circ}$  through ground observations, while Thomas et al. (1997) estimated Vesta's rotational pole coordinates at right ascension  $308^{\circ} \pm 10^{\circ}$  and declination  $48^{\circ} \pm 10^{\circ}$  using Hubble Space Telescope imagery. Müller et al. (2017) further constrained Ryugu's rotational axis to right ascension  $310^{\circ}$ – $340^{\circ}$  and declination  $-40^{\circ} \pm 15^{\circ}$  by combining Herschel Space Observatory data with ground-based light curve analysis. These results typically exhibit  $3^{\circ}$ – $10^{\circ}$  uncertainties, failing to meet sub-pixel-level accuracy requirements for high-resolution remote sensing image registration and three-dimensional reconstruction.

---

\* Corresponding author

The limitations of traditional methods become particularly pronounced when investigating smaller celestial targets. In the context of asteroid exploration missions targeting small size celestial bodies, ground-based observation methods may become entirely ineffective or yield significant errors due to resolution limitations. Systematic deviations in the transformation between the inertial frame and the body-fixed frame, induced by imprecise rotation parameters, would progressively degrade critical mission operations including three-dimensional modelling, landing site selection, and autonomous navigation (Tsuda et al., 2020).

The organization of this paper is as follows: Section 2 describes the refinement method based on the principle of minimizing the residuals of forward intersection. Section 3 details the experimental evaluation of the proposed method, which utilizes remote sensing images of three asteroids (Ceres, Vesta, and Ryugu). Section 4 presents the conclusions and discussions.

## 2. Method

### 2.1 Geometric model construction

When conducting an exploration mission for a celestial body, it is essential to first establish a body-fixed frame (Archinal et al., 2018; Zeitler and Oberst, 1999). The planetary coordinate system

is determined by two factors: the celestial body's mean rotation axis and the definition of longitude specific to the body. For most celestial bodies, the longitude system has been established by referencing surface features (e.g., craters) as fiducial markers (Gehrels, 1967). Generally, the methodology for defining asteroid rotation parameters is illustrated in Figure 1. Using the J2000 mean equatorial plane as the reference Earth equatorial plane, the mean vernal equinox is designated as point  $\lambda$ . The coordinates  $(\alpha_0, \beta_0)$  represent the J2000 equatorial coordinates of the asteroid's north pole. The intersection of the asteroid's equatorial plane with the J2000 mean equatorial plane occurs at two nodes with right ascension values  $\alpha_0 \pm 90^\circ$ . The ascending node at  $\alpha_0 + 90^\circ$  is defined as point M, while the angle between the asteroid's equatorial plane and the J2000 mean equatorial plane is  $90^\circ - \beta_0$ . The prime meridian of the asteroid is established by the intersection of its equatorial plane with its prime meridian, labelled as point N. The position of the prime meridian is determined by the angular distance W, measured eastward along the asteroid's equator from point M to point N.

In the J2000 mean equatorial coordinate system, the orientation of an asteroid is determined by three rotation angles:  $\alpha_0 + 90^\circ$ ,  $90^\circ - \beta_0$  and W. The direction of the asteroid's north pole is defined by  $(\alpha_0, \beta_0)$ , while the orientation of its prime meridian is specified by the angle W.

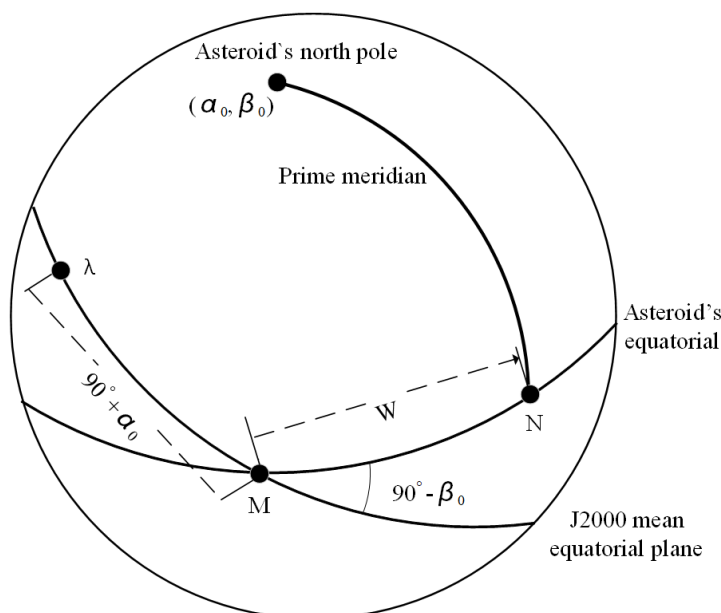


Figure 1 Definition of asteroid rotation parameters and establishment of coordinate system.

The coordinate transformation from the J2000 inertial frame to the asteroid body-fixed frame involves a rotational transformation, governed by the following formula:

$$\begin{bmatrix} X \\ Y \\ Z \end{bmatrix}_{\text{Asteroid}} = R_{J2000}^{\text{Asteroid}} \begin{bmatrix} X \\ Y \\ Z \end{bmatrix}_{J2000} \quad (1)$$

In the above equation,  $R_{J2000}^{\text{Asteroid}}$  denotes the rotation matrix from the J2000 inertial frame to the asteroid body-fixed frame. Following the definition illustrated in Figure 1, this matrix can be expressed as:

$$R_{J2000}^{\text{Asteroid}} = R_Z(W)R_X(90^\circ - \beta_0)R_Z(\alpha_0 + 90^\circ) \quad (2)$$

The imaging geometric model of asteroid remote sensing is utilized to describe the coordinate transformation relationship between image points and ground points, serving as the cornerstone for photogrammetric processing of on-orbit remote sensing images. The rigorous geometric model, based on the collinearity equation, reconstructs the geometric positional relationship of imaging light rays based on imaging principles, thereby establishing the correspondence between image points and object points. By incorporating the transformation relationships among the camera, satellite, and star tracker, the rigorous geometric model of asteroid remote sensing images is expressed as follows:

$$\begin{bmatrix} X \\ Y \\ Z \end{bmatrix} = \begin{bmatrix} X_S \\ Y_S \\ Z_S \end{bmatrix} + \lambda R_{J2000}^{\text{Asteroid}} R_{Star}^{J2000} R_{Body}^{\text{Star}} R_{Cam}^{\text{Body}} \begin{bmatrix} x_c \\ y_c \\ -f \end{bmatrix} \quad (3)$$

where  $(X, Y, Z)$  represent the coordinates of the object point in the asteroid body-fixed frame;  $(X_s, Y_s, Z_s)$  denote the coordinates of the perspective center in the asteroid body-fixed system, corresponding to the exterior orientation linear elements;  $\lambda$  is a scale factor;  $R_{Cam}^{Body}$  denotes the rotation matrix transforming coordinates from the camera frame to the satellite body frame;  $R_{Body}^{Star}$  represents the rotation matrix from the satellite body frame to the star tracker frame;  $R_{Star}^{J2000}$  is the attitude matrix derived from the star tracker measurements in the inertial frame;  $R_{J2000}^{Asteroid}$  defines the rotation matrix from the J2000 inertial frame to the asteroid body-fixed frame;  $(x_c, y_c)$  and  $f$  are the distortion-corrected image coordinates and the camera focal length, respectively.

In this framework,  $R_{Cam}^{Body}$  and  $R_{Body}^{Star}$  are constant matrices calibrated in laboratory settings;  $R_{Star}^{J2000}$  is derived from the attitude determination data of the star tracker. For photogrammetric processing of asteroid remote sensing images, if the asteroid's rotation parameters (e.g.,  $\alpha_0, \beta_0, W$ ) are sufficiently accurate,  $R_{J2000}^{Asteroid}$  can be directly calculated. But when the rotation parameters are unknown or insufficiently precise, the imaging geometric model must incorporate the asteroid's right ascension ( $\alpha_0$ ), declination ( $\beta_0$ ), and rotation period as variables.

By integrating Equations (1) and (2) with Equation (3), the rigorous imaging geometric model incorporating asteroid rotation parameters is formulated as follows:

$$\begin{bmatrix} X \\ Y \\ Z \end{bmatrix} = \begin{bmatrix} X_s \\ Y_s \\ Z_s \end{bmatrix} + \lambda R_Z(W) R_X(90^\circ - \beta_0) R_Z(\alpha_0 + 90^\circ) R_{Star}^{J2000} R_{Body}^{Star} R_{Cam}^{Body} \begin{bmatrix} x_c \\ y_c \\ -f \end{bmatrix} \quad (4)$$

## 2.2 Refinement method

Space probes usually carry payloads such as optical cameras, laser scanners to map the topography and landforms of the celestial bodies (Lauretta et al., 2015). Thus, the rotation parameters can be gradually refined during the on-orbit exploration stage. In this paper, a preliminary refinement method of asteroid's rotation parameters based on photogrammetric processing of remote sensing images is proposed. Determination of the rotation parameters is achieved by minimizing the forward intersection residuals of stereo images through the "brute-force" search. The detailed processing steps are explained in Figure 2. First, the on-orbit remote sensing images of asteroids are pre-processed (e.g., image format conversion and attaching SPICE kernels). Based on the attached SPICE kernels, the initial spacecraft's position and camera pointing's information in inertial frame can be derived (Acton, 1996). Then, the stereopairs are matched using SIFT (Scale-Invariant Feature Transform) method, and a large number of tie points are obtained for each stereopair. Next, given an initial value of the rotation parameters that can be obtained from ground-based observation or can be specified as any number, a series of combinations of right ascension and declination can be obtained by sampling around the initial value at certain intervals (e.g., 5 degrees) within a certain search range (e.g.,  $\pm 50$  degrees). Using each right ascension and declination's combination, the Exterior Orientations (EO) of stereopairs are converted from the inertial frame to the body-fixed frame. Then, the matched tie points and the converted EO parameters of the stereopairs are utilized to perform the forward intersection, which results in the ground point coordinates of tie points and the corresponding intersection residuals. For a stereopair, the Root Mean Square Error (RMSE) of the intersection residuals for all tie points can be computed. In the next round, a smaller interval (e.g., 1 degree) and search range (e.g.,  $\pm 5$  degrees) can be adopted to further refine the rotation parameters. In this way, multiple rounds of refinement are carried out.

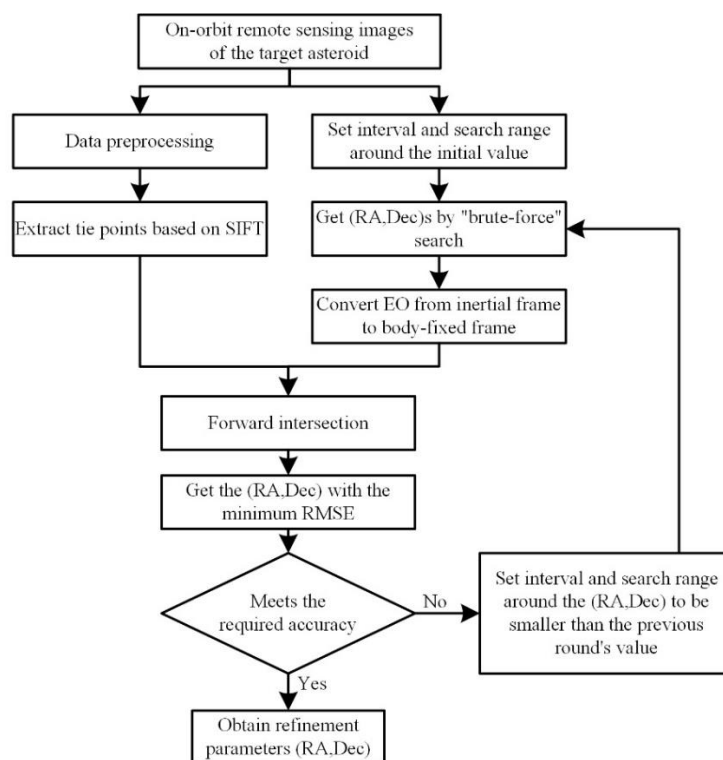


Figure 2 Initial refinement process for rotation parameters  
(RA = right ascension; Dec = declination)

### 3. Results

#### 3.1 Test Datasets

To validate the feasibility of the proposed method, this study conducted experiments using on-orbit remote sensing images of three distinct asteroids: Ceres, Vesta, and Ryugu. For Ryugu, twenty experimental images captured by the Hayabusa-2 Optical Navigation Camera-Telescopic (ONC-T) on July 10, 2018 were selected. Similarly, Ceres images were acquired during the Survey phase on June 6, 2015 using the Dawn spacecraft's Framing Camera (FC), while Vesta images were acquired from the Approach phase on December 2, 2011, captured by the same Framing Camera instrument. The information of the images of the three asteroids is presented in Table 1.

Table 1 Information of the images selected for experiment.

Asteroid Name	Task Phase	Altitude (km)	Resolution (m/pixel)
Ceres	Survey	4853 - 4869	409 - 411
Vesta	Approach	5487 - 5493	487 - 488
Ryugu	Home Position Arrival	19.90 - 19.93	2.10 - 2.13

#### 3.2 Image Matching Results

The tie points were firstly obtained by SIFT feature matching methods. Then, RANSAC (RANdom SAMple Consensus) method is used to remove the outliers. The experiments were designed as follows: Twenty images from each asteroid datasets were selected for refining the rotation parameters. The Ceres dataset yielded 85 valid feature correspondences, while both Ryugu and Vesta groups generated 112 robust matching pairs, with their spatial distributions illustrated in Figure 3-Figure 5.

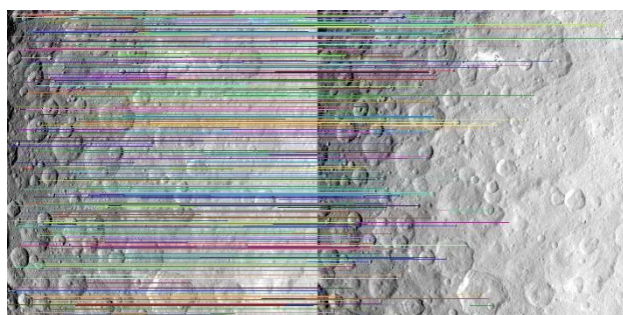


Figure 3 Matching results from the Survey detection phase of Ceres images.

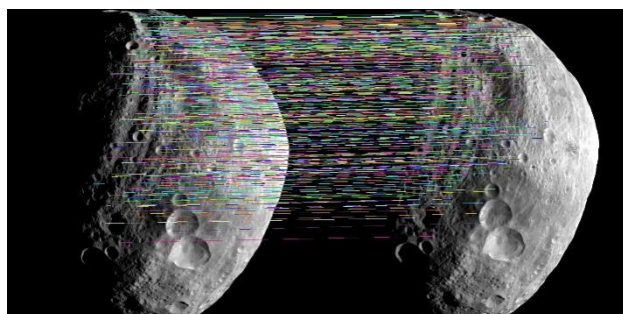


Figure 4 Matching results from the Approach detection phase of Vesta images.

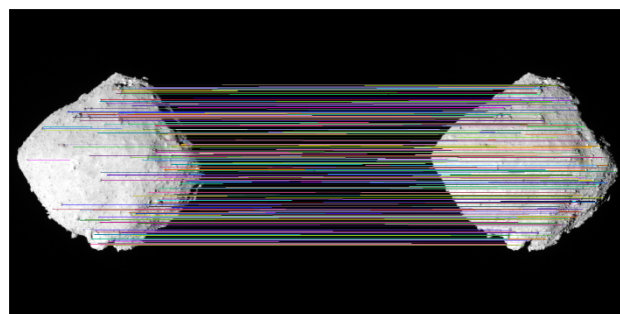


Figure 5 Matching results from the Home Position Arrival detection phase of Ryugu images.

#### 3.3 Refinement results

To resolve the challenge of unknown rotational axis orientation, this study proposes a three-stage hierarchical optimization strategy leveraging high-precision spacecraft attitude and orbital data. The methodological framework operates as follows:

##### 1. Coarse Global Search Phase

Initial parameter spaces span the complete celestial sphere: Right Ascension (RA:  $0^{\circ}$ - $360^{\circ}$ ) and Declination (Dec:  $-90^{\circ}$ - $90^{\circ}$ ), sampled at  $20^{\circ}$  grid intervals is used for coarse global search. Intersection quality is evaluated through root mean square error (RMSE) of forward intersection residuals, with the sub-region exhibiting minimum RMSE values advancing to subsequent optimization.

##### 2. Meso-scale Refinement Phase

Centered on the determined parameters from Stage 1, this phase implements  $5^{\circ}$  grid sampling to establish sub-regional optimal solution.

##### 3. Final Optimization Phase

Final optimization employs  $1^{\circ}$  grid increments within the meso-scale solution domain.

Figure 6-Figure 8 shows the three-round refinement processes of Ceres, Vesta and Ryugu, the determined rotation parameters based on the proposed method of three asteroids are shown in Table 2. The center of the ellipses represents the selected coordinates of Right Ascension and Declination, and the radius represents the residual of the forward intersection. The three experimental datasets presented in Figure 6-Figure 8 demonstrate that two characteristic regions emerge during the initial phase of each experiment, where the root mean square error (RMSE) values exhibit a convergent spatial distribution toward central points. Spatial coordinates are calculated through the forward intersection method, and then the asteroid's radius is derived. By comparing this calculated radius with the known radius of the asteroid, the region where the true value lies can be selected for the next - round refinement.

Table 2 Preliminary refinement results

Asteroid Name	Prior Value	Refinement Result	Value from SPICE
Ceres	RA $333^{\circ} \pm 2^{\circ}$	$291^{\circ}$	$291.418^{\circ}$
	Dec $43^{\circ} \pm 2^{\circ}$	$67^{\circ}$	$66.764^{\circ}$
Vesta	RA $308^{\circ} \pm 10^{\circ}$	$309^{\circ}$	$309.031^{\circ}$
	Dec $48^{\circ} \pm 10^{\circ}$	$42^{\circ}$	$42.235^{\circ}$
Ryugu	RA $310^{\circ} \sim 340^{\circ}$	$97^{\circ}$	$96.431^{\circ}$
	Dec $-40^{\circ} \pm 15^{\circ}$	$-67^{\circ}$	$-66.387^{\circ}$



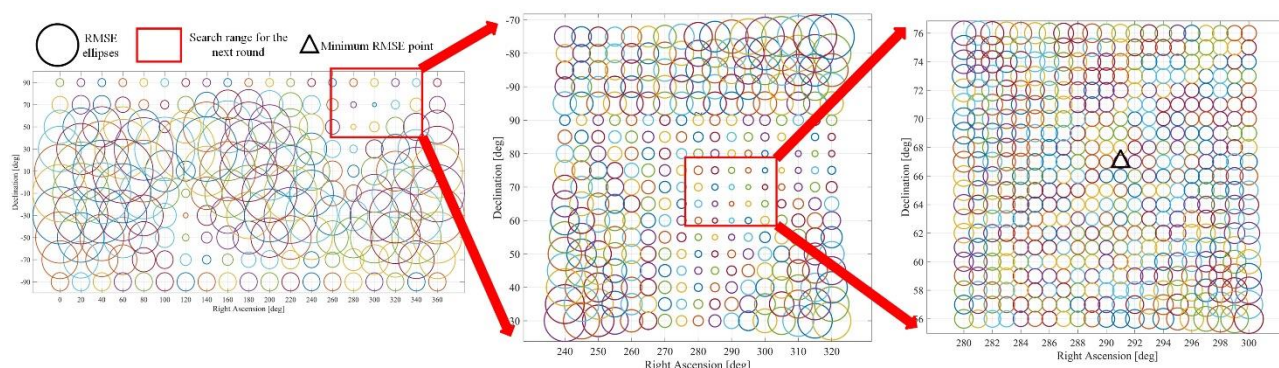


Figure 6 Refinement process of Ceres rotation parameters

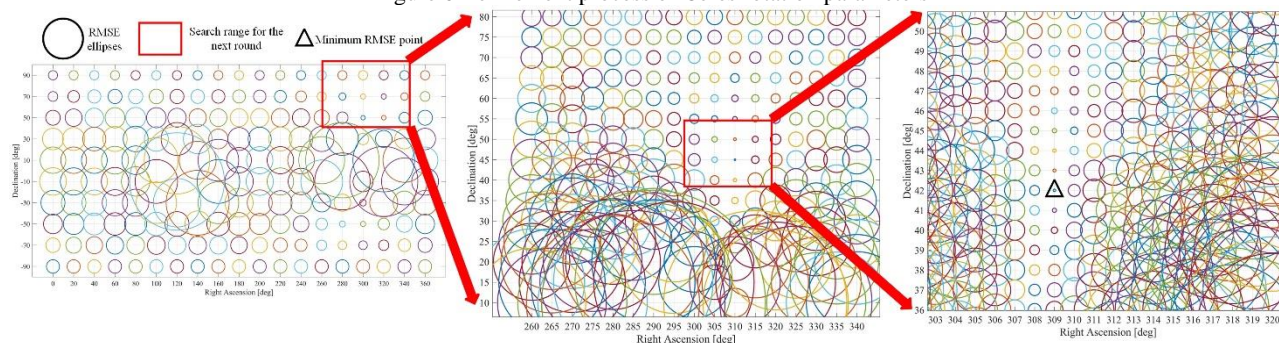


Figure 7 Refinement process of Vesta rotation parameters

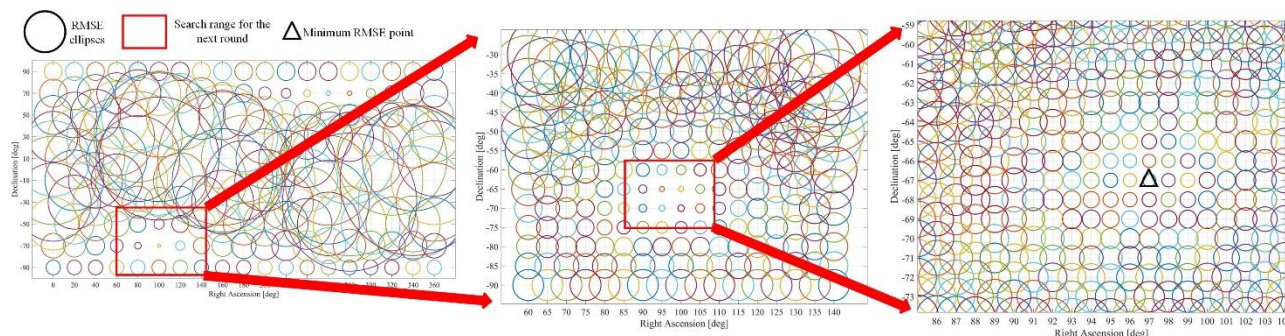


Figure 8 Refinement process of Ryugu rotation parameters

### 3.4 Refined results with random errors added

Building upon preliminary refinement experiments, this study further conducted refined experiments incorporating random initial orbit-determination errors to better align with practical exploration scenarios and evaluate the robustness of the proposed method. A secondary sampling process with one-degree intervals was performed around the refined results in the J2000 inertial reference frame to further test the stability of this method. This procedure involved progressively introducing random perturbations to the image positions, followed by systematic evaluation of forward intersection residuals across the parameter space. The optimal right ascension and declination combination was subsequently determined by identifying the minimum residual configuration through this localized grid search (Figure 9-Figure 14). The values used for comparison are from the SPICE values (Acton, 1996). The experimental results demonstrate a certain degree of tolerance of our method to initial orbit determination errors. These experiments demonstrate that the proposed methodology maintains effective refinement of asteroid

rotation parameters even with some initial positioning biases, confirming its practical applicability and operational reliability in real scenarios.

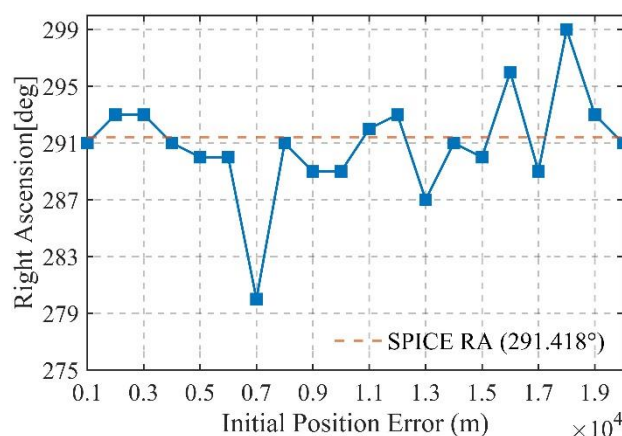


Figure 9 Refinement results of the Right Ascension of Ceres under initial orbit - determination errors



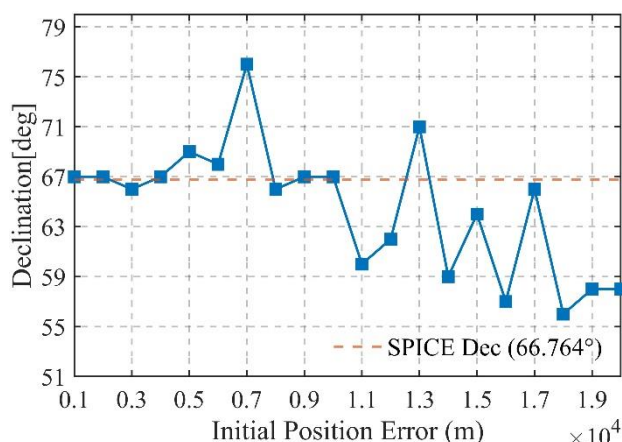


Figure 10 Refinement results of the Declination of Ceres under initial orbit - determination errors

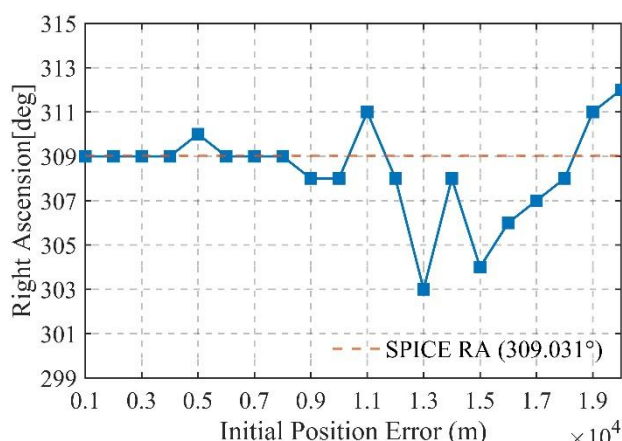


Figure 11 Refinement results of the Right Ascension of Vesta under initial orbit - determination errors

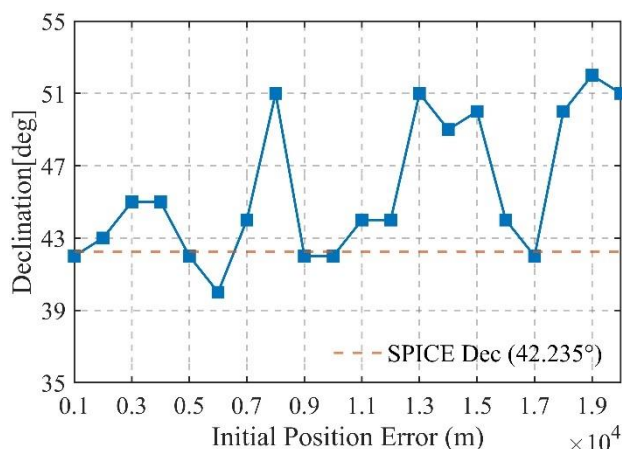


Figure 12 Refinement results of the Declination of Vesta under initial orbit - determination errors

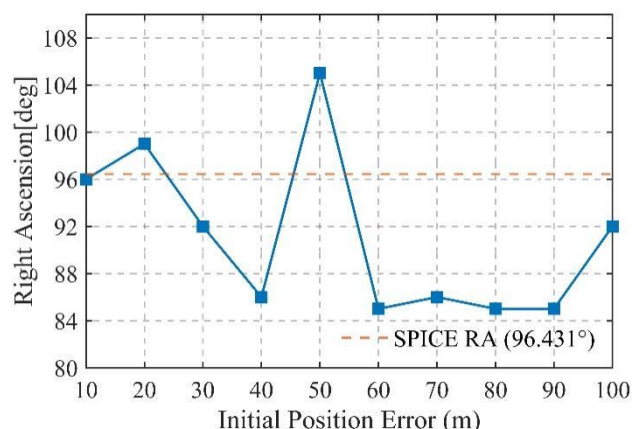


Figure 13 Refinement results of the Right Ascension of Ryugu under initial orbit - determination errors

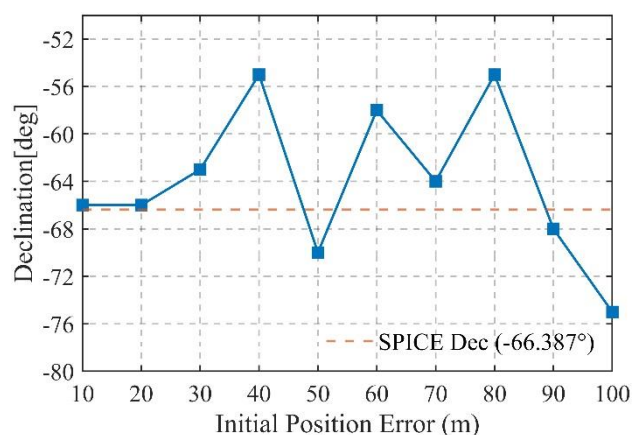


Figure 14 Refinement results of the Declination of Ryugu under initial orbit - determination errors

#### 4. Conclusions

This study proposes a preliminary refinement method for asteroid rotation parameters utilizing on-orbit remote sensing images. A camera model with right ascension and declination was established. Based on the principle of minimizing the forward intersection residuals, a preliminary right ascension and declination can be determined with a relatively coarse accuracy. Experimental validation using on-orbit images of Ceres, Vesta, and Ryugu demonstrated the robustness and universality of the proposed method. The three-stage hierarchical optimization strategy effectively refined rotation parameters while maintaining stability under initial orbital determination errors. However, limitations persist. The brute-force search efficiency requires optimization, and the simulated error scenarios may not fully reflect the various error effects in deep-space exploration missions. In addition, we used the reconstructed level SPICE kernels to construct the camera model. Thus, the accuracy of the proposed method heavily depends on the quality of the SPICE data. It should be noted that the determined rotation parameters by the proposed method is a preliminary refinement method, which can be used as inputs for high accuracy refinement method such as bundle adjustment.

#### Acknowledgements

This research was funded by the Space Optoelectronic Measurement and Perception Lab, Beijing Institute of Control Engineering, grant number LabSOMP-2023-07; and the National Natural Science Foundation of China, grant number 42241147;

and the Open Program of Collaborative innovation Center of GeoInformation Technology for Smart Central Plains Henan Province, grant number 2023C002.

## References

- Acton, C.H., 1996. Ancillary data services of NASA's Navigation and Ancillary Information Facility. *Planet. Space Sci.* 44, 65–70. [https://doi.org/10.1016/0032-0633\(95\)00107-7](https://doi.org/10.1016/0032-0633(95)00107-7)
- Archinal, B.A., Acton, C.H., A'Hearn, M.F., Conrad, A., Consolmagno, G.J., Duxbury, T., Hestroffer, D., Hilton, J.L., Kirk, R.L., Klioner, S.A., McCarthy, D., Meech, K., Oberst, J., Ping, J., Seidelmann, P.K., Tholen, D.J., Thomas, P.C., Williams, I.P., 2018. Report of the IAU Working Group on Cartographic Coordinates and Rotational Elements: 2015. *Celest. Mech. Dyn. Astron.* 130, 22. <https://doi.org/10.1007/s10569-017-9805-5>
- Burmeister, S., Willner, K., Schmidt, V., Oberst, J., 2018. Determination of Phobos' rotational parameters by an inertial frame bundle block adjustment. *J. Geod.* 92, 963–973. <https://doi.org/10.1007/s00190-018-1112-8>
- Drummond, J.D., Fugate, R.Q., Christou, J.C., Hege, E.K., 1998. Full adaptive optics images of asteroids ceres and vesta; rotational poles and triaxial ellipsoid dimensions. *Icarus* 132, 80–99. <https://doi.org/10.1006/icar.1997.5882>
- Gehrels, T., 1967. Minor planets. I. The rotation of Vesta. *Astron. J.* 72, 929. <https://doi.org/10.1086/110364>
- Konopliv, A.S., Sjogren, W.L., 1995. The JPL mars gravity field, Mars50c, based upon viking and mariner 9 doppler tracking data (No. NASA-CR-198881).
- Lauretta, D.S., Balram-Knutson, S.S., Beshore, E., Boynton, W.V., Drouet d'Aubigny, C., DellaGiustina, D.N., Enos, H.L., Golish, D.R., Hergenrother, C.W., Howell, E.S., Bennett, C.A., Morton, E.T., Nolan, M.C., Rizk, B., Roper, H.L., Bartels, A.E., Bos, B.J., Dworkin, J.P., Highsmith, D.E., Lorenz, D.A., Lim, L.F., Mink, R., Moreau, M.C., Nuth, J.A., Reuter, D.C., Simon, A.A., Bierhaus, E.B., Bryan, B.H., Ballouz, R., Barnouin, O.S., Binzel, R.P., Bottke, W.F., Hamilton, V.E., Walsh, K.J., Chesley, S.R., Christensen, P.R., Clark, B.E., Connolly, H.C., Crombie, M.K., Daly, M.G., Emery, J.P., McCoy, T.J., McMahon, J.W., Scheeres, D.J., Messenger, S., Nakamura-Messenger, K., Righter, K., Sandford, S.A., 2017. OSIRIS-REx: sample return from asteroid (101955) bennu. *Space Sci. Rev.* 212, 925–984. <https://doi.org/10.1007/s11214-017-0405-1>
- Lauretta, D.S., Bartels, A.E., Barucci, M.A., Bierhaus, E.B., Binzel, R.P., Bottke, W.F., Campins, H., Chesley, S.R., Clark, B.C., Clark, B.E., Cloutis, E.A., Connolly, H.C., Crombie, M.K., Delbó, M., Dworkin, J.P., Emery, J.P., Glavin, D.P., Hamilton, V.E., Hergenrother, C.W., Johnson, C.L., Keller, L.P., Michel, P., Nolan, M.C., Sandford, S.A., Scheeres, D.J., Simon, A.A., Sutter, B.M., Vokrouhlický, D., Walsh, K.J., 2015. The OSIRIS-REx target asteroid (101955) Bennu: Constraints on its physical, geological, and dynamical nature from astronomical observations. *Meteorit. Planet. Sci.* 50, 834–849. <https://doi.org/10.1111/maps.12353>
- Miller, J.K., Konopliv, A.S., Antreasian, P.G., Bordi, J.J., Chesley, S., Helfrich, C.E., Owen, W.M., Wang, T.C., Williams, B.G., Yeomans, D.K., Scheeres, D.J., 2002. Determination of shape, gravity, and rotational state of asteroid 433 eros. *Icarus* 155, 3–17. <https://doi.org/10.1006/icar.2001.6753>
- Müller, T.G., Ďurech, J., Ishiguro, M., Mueller, M., Krühler, T., Yang, H., Kim, M.-J., O'Rourke, L., Usui, F., Kiss, C., Altieri, B., Carry, B., Choi, Y.-J., Delbo, M., Emery, J.P., Greiner, J., Hasegawa, S., Hora, J.L., Knust, F., Kuroda, D., Osip, D., Rau, A., Rivkin, A., Schady, P., Thomas-Osip, J., Trilling, D., Urakawa, S., Vilenius, E., Weissman, P., Zeidler, P., 2017. Hayabusa-2 mission target asteroid 162173 Ryugu (1999 JU3): Searching for the object's spin-axis orientation. *Astron. Astrophys.* 599, A103. <https://doi.org/10.1051/0004-6361/201629134>
- Preusker, F., Scholten, F., Matz, K.-D., Elgner, S., Jaumann, R., Roatsch, T., Joy, S.P., Polanskey, C.A., Raymond, C.A., Russell, C.T., 2016. Dawn at ceres — shape model and rotational state 1954.
- Preusker, F., Scholten, F., Matz, K.-D., Roatsch, T., Willner, K., Hviid, S.F., Knollenberg, J., Jorda, L., Gutiérrez, P.J., Kührt, E., Mottola, S., A'Hearn, M.F., Thomas, N., Sierks, H., Barbieri, C., Lamy, P., Rodrigo, R., Koschny, D., Rickman, H., Keller, H.U., Agarwal, J., Barucci, M.A., Bertaux, J.-L., Bertini, I., Cremonese, G., Deppo, V.D., Davidsson, B., Debei, S., Cecco, M.D., Fornasier, S., Fulle, M., Groussin, O., Güttler, C., Ip, W.-H., Kramm, J.R., Küppers, M., Lara, L.M., Lazzarin, M., Moreno, J.J.L., Marzari, F., Michalik, H., Naletto, G., Oklay, N., Tubiana, C., Vincent, J.-B., 2015. Shape model, reference system definition, and cartographic mapping standards for comet 67P/Churyumov-Gerasimenko — Stereo-photogrammetric analysis of Rosetta/OSIRIS image data. *Astron. Astrophys.* 583, A33. <https://doi.org/10.1051/0004-6361/201526349>
- Rayman, M.D., Mase, R.A., 2014. Dawn's exploration of Vesta. *Acta Astronaut.* 94, 159–167. <https://doi.org/10.1016/j.actaastro.2013.08.003>
- Roatsch, Th., Kersten, E., Matz, K.-D., Preusker, F., Scholten, F., Jaumann, R., Raymond, C.A., Russell, C.T., 2017. High-resolution ceres low altitude mapping orbit atlas derived from dawn framing camera images. *Planet. Space Sci.* 140, 74–79. <https://doi.org/10.1016/j.pss.2017.04.008>
- Thomas, P.C., Binzel, R.P., Gaffey, M.J., Storrs, A.D., Wells, E.N., Zellner, B.H., 1997. Impact Excavation on Asteroid 4 Vesta: Hubble Space Telescope Results. *Science* 277, 1492–1495. <https://doi.org/10.1126/science.277.5331.1492>
- Tsuda, Y., Saiki, T., Terui, F., Nakazawa, S., Yoshikawa, M., Watanabe, S., Hayabusa2 Project Team, 2020. Initial Achievements of Hayabusa2 in Asteroid Proximity Phase. *Trans. Jpn. Soc. Aeronaut. Space Sci.* 63, 115–123. <https://doi.org/10.2322/tjsass.63.115>
- Tsuda, Y., Yoshikawa, M., Saiki, T., Nakazawa, S., Watanabe, S., 2019. Hayabusa2—sample return and kinetic impact mission to near-earth asteroid ryugu. *Acta Astronaut.* 156, 387–393. <https://doi.org/10.1016/j.actaastro.2018.01.030>
- Zeitler, W., Oberst, J., 1999. The Mars pathfinder landing site and the viking control point network. *J. Geophys. Res. Planets* 104, 8935–8941. <https://doi.org/10.1029/98JE01430>